Kinetics, Mechanism, and Thermodynamics of Glyoxal–S(IV) Adduct Formation

Terese M. Olson and Michael R. Hoffmann*

Environmental Engineering Science, W. M. Keck Laboratories, California Institute of Technology, Pasadena, California 91125 *(Received: April 30, 1987; In Final Form: June 29, 1987)*

The reversible addition of glyoxal (ethanedial) and S(IV) to form glyoxal monobisulfite (GMBS) was studied spectrophotometrically over the pH range of 0.7–3.3. Far from equilibrium, the rate of GMBS formation is given by $d[GMBS]/dt = (k_{1,app}\alpha_1 + k_{2,app}\alpha_2)[C_2H_2O_2][S(IV)]$, where $[C_2H_2O_2] = [(CH(OH)_2)_2] + [CH(OH)_2CHO] + [CHOCHO]$, $[S(IV)] = [H_2O{\cdot}SO_2] + [HSO_3^-] + [SO_3^{2-}]$, $\alpha_1 = [HSO_3^-]/[S(IV)]$, and $\alpha_2 = [SO_3^{2-}]/[S(IV)]$. The apparent rate constants, $k_{1,app} = 0.13\ M^{-1}\ s^{-1}$ and $k_{2,app} = 2.08 \times 10^3\ M^{-1}\ s^{-1}$, are pH independent functions of the dehydration equilibrium constants of $(CH(OH)_2)_2$ and $CHOCH(OH)_2$, and intrinsic rate constants for the reaction of HSO_3^- and SO_3^{2-} with unhydrated and singly hydrated glyoxal. Glyoxal dibisulfite (GDBS) and GMBS were shown to dissociate with a rate given by $d[S(IV)]/dt = \{k'_{-1} + k''_{-1}K_{D3} + (k'_{-2}K'_{a2} + k''_{-2}K''_{a2}K_{D3})/\{H^+\}\}[GMBS]_t + \{k_{-3} + k_{-4}K_{a3}/\{H^+\}\}[GDBS]_t$, where k_{-1} and k_{-2} correspond to the release of bisulfite and sulfite, respectively, from unhydrated and hydrated GMBS species; k_{-3} and k_{-4} correspond to the release of bisulfite and sulfite from GDBS; K_{D3} is the dehydration constant for GMBS; and K'_{a2}, K''_{a2}, and K_{a3} are acid dissociation constants. Stability constants for the formation of GMBS and GDBS were determined to be ${}^cK_1 = [CH(OH)_2CH(OH)SO_3^-]/([CH(OH)_2)_2][HSO_3^-]) = 2.81 \times 10^4\ M^{-1}$ and ${}^cK_2 = [(CH(OH)SO_3^-)_2]/([CH(OH)_2CH(OH)SO_3^-][HSO_3^-]) = 1.45 \times 10^4\ M^{-1}$ at 25 °C and $\mu = 0.2$ M.

Introduction

Aldehyde–bisulfite adducts are believed to form at appreciable concentrations in atmospheric water droplets of polluted environments and are thought to play an important role in stabilizing SO_2 in the aqueous phase.[1,2] To predict which aldehydes represent significant S(IV) reservoirs, we have previously examined the formation kinetics and stability of formaldehyde–, benzaldehyde–, methylglyoxal–, acetaldehyde–, and hydroxyacetaldehyde–S(IV) adducts.[3-5] Formaldehyde and methylglyoxal (CH_3COCHO), which both have large effective Henry's law constants, were found to form highly stable S(IV) addition compounds and are likely to be important when they are present in the environment. Conversely, hydroxyphenylmethanesulfonate, the benzaldehyde adduct, will be much less important since it is less stable and since benzaldehyde is predominantly unhydrated (hence it is unlikely to have a large Henry's law constant).

The objective of this work has been to investigate the reaction of S(IV) with another predominantly hydrated α-dicarbonyl, glyoxal (ethanedial, CHOCHO). Recent experimental evidence has shown that dicarbonyls such as glyoxal and methylglyoxal are primary gas-phase oxidation products of aromatic hydrocarbons after free-radical attack.[6a,b] Theoretical calculations by Calvert and Madronich[7] suggest that α-dicarbonyls account for a substantial mole fraction of the initial oxidation product distribution of an aromatic hydrocarbon mixture. Dicarbonyls, including glyoxal, have also been identified in fog- and rainwater samples.[8]

Only one determination of the stability constants for the glyoxal mono- and dibisulfite adducts, 1-hydroxy-2,2-diol-ethanesulfonate and 1,2-dihydroxy-1,2-ethanedisulfonate (hereafter respectively denoted with the acronyms GMBS and GDBS) is known. Salomaa reported a value of the apparent stability constant of GDBS as $3.7 \times 10^3\ M^{-1}$ at pH 7.3 and an unspecified ionic strength, and that the formation constant for GMBS must be greater than $3.7 \times 10^3\ M^{-1}$.[9] He also described the kinetics of the addition of sulfite to the first glyoxal carbonyl group as being comparable to the rate of addition of formaldehyde and sulfite.

Since the pH conditions of fogs, clouds, and haze aerosols are typically acidic, the kinetic and thermodynamic parameters obtained in this work were determined at pH ≤ 4.0. Conventional and stopped-flow spectrophotometric methods were employed to obtain the rate constants for adduct formation (GMBS only) and dissociation (GMBS and GDBS). Spectrophotometry was also used to determine the successive adduct stability constants. An independent calculation of the stability constant for GMBS was possible from the ratio of forward/reverse rate constants.

Experimental Procedures

Materials. Stock solutions of glyoxal were prepared from a 40% reagent grade glyoxal-in-water solution (Aldrich) which was periodically filtered and standardized by an alkalimetric titration technique described by Salomaa.[9] The filtering step was necessary to remove the solid polymer which formed slowly at room temperature. Since the depolymerization process was apparently quite slow, buffered or acidified glyoxal stock solutions (at approximately twice the sample concentration) were heated to 35 °C for 30 min and allowed to stand for several days in a N_2-atmosphere glovebox before use. Buffer solutions were prepared with reagent grade sodium hydroxide (Baker), hydrochloric acid (Baker), chloroacetic acid (Kodak), dichloroacetic acid (MCB), phosphoric acid (Spectrum), sodium acetate (Baker), glacial acetic acid (Mallinckrodt), and monobasic potassium phosphate (Baker). Small amounts of disodium EDTA were added to the buffers to inhibit possible metal-catalyzed oxidation of S(IV).

The disodium salt of the glyoxal–bisulfite addition compound was synthesized and recrystallized by using a method adapted from Ronzio and Waugh.[10] Based on an elemental analysis of the salt (Galbraith Laboratories), its stoichiometry was $(NaCH(OH)SO_3)_2{\cdot}H_2O$.

Stock S(IV) solutions were prepared fresh before use from A.R. grade disodium sulfite (Baker). All solutions were prepared in a glovebox with deoxygenated, 18 MΩ·cm resistivity water (Millipore). Oxygen was purged by degassing with high-purity N_2 gas. Ionic strength was held constant at $\mu = 0.2$ M with sodium chloride.

Methods. The kinetics of adduct formation was studied by monitoring the disappearance of free S(IV) (i.e., $H_2O{\cdot}SO_2$, HSO_3^-, and SO_3^{2-}) at 280 nm ($\lambda_{max,H_2O{\cdot}SO_2}$) with a Hewlett-Packard Model 8450A UV/vis spectrophotometer linked to an IBM Model XT

(1) Munger, J. W.; Tiller, C.; Hoffmann, M. R. *Science* **1986**, *231*, 247-49.
(2) Ang, C. C.; Lipari, F.; Swarin, S. W. *Environ. Sci. Technol.* **1987**, *21*, 102-5.
(3) Boyce, S. D.; Hoffmann, M. R. *J. Phys. Chem.* **1984**, *88*, 4740-46.
(4) Olson, T. M.; Boyce, S. D.; Hoffmann, M. R. *J. Phys. Chem.* **1986**, *90*, 2482-88.
(5) (a) Betterton, E. A.; Hoffmann, M. R. *J. Phys. Chem.* **1987**, *91*, 3011-20. (b) Betterton, E. A.; Hoffmann, M. R., submitted for publication in *Environ. Sci. Technol.*
(6) (a) Tuazon, E. C.; Atkinson, R.; MacLeod, H.; Biermann, H. W.; Winer, A. M.; Carter, W. P. L.; Pitts, J. N. *Environ. Sci. Technol.* **1984**, *18*, 981-84. (b) Tuazon, E. C.; MacLeod, H.; Atkinson, R.; Carter, W. P. L. *Environ. Sci. Technol.* **1986**, *20*, 383-87.
(7) Calvert, J. G.; Madronich, S. *J. Geophys. Res.* **1987**, *92*, 2211-20.
(8) Steinberg, S.; Kaplan, I. R. *Int. J. Environ. Anal. Chem.* **1984**, *18*, 253-66.
(9) Salomaa, P. *Acta Chem. Scand.* **1956**, *10*, 306-10.
(10) Ronzio, A. R.; Waugh, T. D. *Org. Synth.* **1944**, Collect. Vol. 3, 438-40.

0022-3654/88/2092-0533$01.50/0

computer. The quartz, 10 cm reaction cell was water-jacketed and a Haake water recirculation bath was used to maintain a constant temperature of 25 °C. Usually four replications were performed at each pH with a minimum of 200 absorbance measurements being collected in each data set.

Adduct dissociation was studied indirectly by dissolving the salt of the addition compound, mixing this fresh solution with a pH-buffered iodine solution (containing excess KI) and monitoring the disappearance of triiodide at 351 nm (λ_{max} for I_3^-). Since the oxidation reaction of S(IV) to S(VI) by iodine is extremely rapid, the rate of disappearance of iodine therefore is equal to the rate of liberation of free S(IV). At pH 1.3 and 1.8 absorbance measurements of aliquots were taken manually in a 1-cm cell over several days. Between pH 1.8 and 5.0, the reaction was conducted directly in a 1-cm mixing cell and continuous absorbance measurements were made. Cell temperature (25 °C) was maintained with a Hewlett-Packard Model 89100A temperature controller. Above pH 5.0, the reaction was studied by using a stopped-flow spectrophotometer (Dionex). In these experiments, buffered I_2/KI solutions were placed in one syringe while freshly prepared GDBS solutions (acidified to approximately pH 2) were placed in another. Acidification of the adduct reagent was necessary to quench the dissociation rate of the adduct. The pH of the reaction mixture was determined by analyzing samples of the stopped-flow effluent stream. No loss of iodine was evident in the absence of S(IV).

The apparent stability constant for GMBS, K_1, was determined by three independent methods. An estimate was first calculated from the previously determined forward and reverse rate constants (method A). A second, direct determination (method B) involved measuring the concentration of unbound S(IV) in equilibrated solutions containing a tenfold excess of glyoxal; the formation of GDBS was thereby minimized. Free S(IV) concentrations were determined by mixing the equilibrated mixture with an acidified I_2/KI solution and spectrophotometrically measuring the residual I_3^- concentration. The change in absorbance at 351 nm relative to light absorption by I_3^- in the absence of S(IV) was used to calculate the amount of I_3^- consumed (i.e., amount of free S(IV) present). Beer's law calibration curves were used to relate light absorption to I_3^- concentrations. Although the pH of the resulting I_2/KI/adduct mixture was approximately 1.7, even slight extents of adduct dissociation which occurred over the initial ~30 s seriously interfered with the measurement. Stopped-flow mixing of the two reagents was therefore employed. During these experiments the stopped-flow apparatus was housed in a N_2-atmosphere glovebox. Stock I_2 solutions were protected from light and analyzed with a primary standard As_2O_3 solution after each experiment.

The third method (method C) involved measuring the concentration of unbound S(IV) in equilibrated solutions of the disodium dibisulfite salt and fitting the single and double association constants to the data with a nonlinear least-squares fitting routine. The technique for determining $[S(IV)]_{unbound}$ was similar to the second method above except that the reagents were mixed in a 1-cm mixing cell and the absorbance due to residual I_3^- was measured by conventional spectrophotometry. Adduct dissociation under these conditions ($[CHOCHO]_{tot}$:$[(S(IV)]_{tot}$ = 1:2) was insignificant even several minutes after mixing.

Results

GMBS Formation Kinetics. Under the imposed condition, $[CHOCHO]_t \gg [S(IV)]_t$, pseudo-first-order plots of ln $\{(A - A_\infty)/(A_0 - A_\infty)\}$ vs time were linear ($r^2 \geq 0.99$) for reaction extents up to 90%. The formation of GMBS is therefore first order with respect to $[S(IV)]_{free}$ (which shall hereafter be denoted simply as [S(IV)]) below pH 3.2. This pseudo-first-order behavior further implies that the amount of GDBS formed was indeed insignificant. The reaction order with respect to glyoxal was examined by varying the aldehyde concentration at constant pH. The pseudo-first-order rate constant, k_{obsd}, exhibited a linear dependence on $[C_2H_2O_2]_t$. Slope values close to unity obtained from logarithmic plots of the data (see Figure 1) demonstrate this relationship.

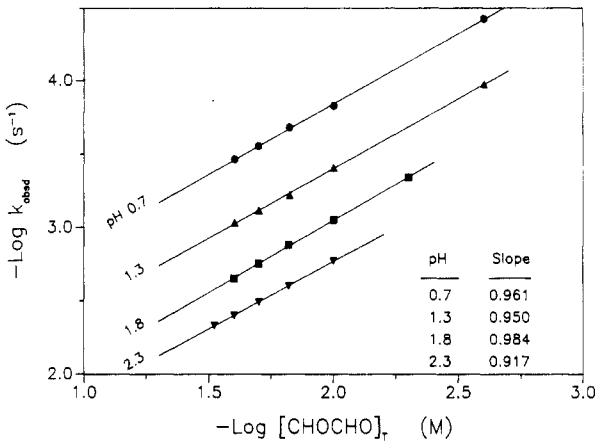

Figure 1. Dependence of pseudo-first-order rate constants for GMBS formation on $[CHOCHO]_t$. Solid lines are linear least-squares fits to the data. Reaction conditions: $[S(IV)]_t$ = 0.1–2.5 mM, T = 25 °C, μ = 0.2 M.

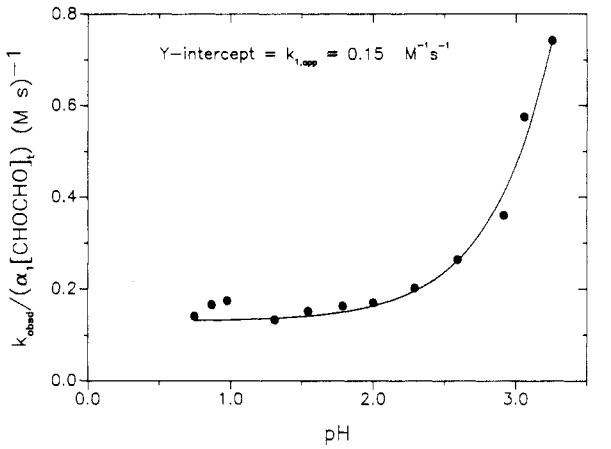

Figure 2. Dependence of $k_{obsd}/(\alpha_1[CHOCHO]_t) = \nu/([HSO_3^-][CHOCHO]_t)$ on pH. Data is taken from Table I.

TABLE I: Kinetic Data for the Formation of Glyoxal Monobisulfite

pH	10^2[CHOCHO], M	10^3[S(IV)], M	$10^3 k_{obsd}$ ($\pm\sigma$), s^{-1}	$10^3 k_{calcd}$, s^{-1}
0.74	2.0	0.15	0.280 (0.005)	0.262
0.87	2.0	0.20	0.331 (0.013)	0.337
0.98	2.0	0.20	0.448 (0.010)	0.420
1.31	2.0	0.20	0.769 (0.042)	0.790
1.55	2.0	0.25	1.25 (0.05)	1.16
1.79	2.0	0.50	1.79 (0.05)	1.65
2.00	2.0	0.50	2.26 (0.12)	2.18
2.29	2.0	1.0	3.21 (0.10)	3.11
2.59	2.0	1.0	4.68 (0.14)	4.63
2.92	2.0	1.0	6.78 (0.15)	7.72
3.06	1.5	1.5	8.26 (0.18)	7.44
3.26	1.5	1.5	10.8 (0.4)	10.8

The pseudo-first-order rate constants obtained as a function of pH are tabulated in Table I. Over the pH range studied, the overall pH dependence of k_{obsd} closely resembled earlier trends established for formaldehyde- and benzaldehyde–S(IV) addition compounds.[3,4] In these studies, the reaction rate increase with increasing pH was explained by two rate-determining steps for adduct formation: the nucleophilic attack by HSO_3^- and SO_3^{2-} on the carbonyl carbon atom. To test whether the data in Table I obeyed such a mechanism, $k_{obsd}/(\alpha_1[CHOCHO]_t) = \nu/[HSO_3^-][CHOCHO]_t$, where $\alpha_1 = [HSO_3^-]/[S(IV)]$, was first plotted against pH (Figure 2). This pseudo-second-order rate constant became invariant below pH 2, suggesting that bisulfite addition is the dominant rate-determining pathway over this pH range. Between pH 2.5 and 3.2, the pseudo-second-order rate constant, $k_{obsd}/[CHOCHO]_t$, was inversely dependent on the hydrogen ion activity as shown in Figure 3. Since the concen-

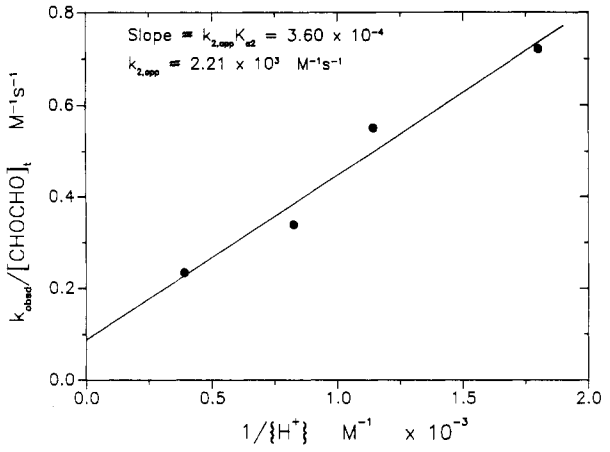

Figure 3. Dependence of $k_{obsd}/[CHOCHO]$ on $1/\{H^+\}$ over pH 2.6–3.2. Solid line represents a linear least-squares fit to the data taken from Table I.

tration of SO_3^{2-} also varies inversely with $\{H^+\}$ over this pH range, a second pathway involving SO_3^{2-} addition is implied. The following reaction mechanism for GMBS formation is therefore proposed for the pH range of 0.7 to 3.2:

$$H_2O{\cdot}SO_2 \overset{K_{a1}}{\rightleftharpoons} H^+ + HSO_3^- \quad \text{(fast)} \qquad (1a)$$

$$HSO_3^- \overset{K_{a2}}{\rightleftharpoons} H^+ + SO_3^{2-} \quad \text{(fast)} \qquad (1b)$$

$$(CH(OH)_2)_2 \overset{K_{D1}}{\rightleftharpoons} CH(OH)_2CHO + H_2O \quad \text{(fast)} \qquad (2a)$$

$$CH(OH)_2CHO \overset{K_{D2}}{\rightleftharpoons} CHOCHO + H_2O \quad \text{(fast)} \qquad (2b)$$

$$CH(OH)_2CHO + HSO_3^- \underset{k'_{-1}}{\overset{k'_1}{\rightleftharpoons}} CH(OH)_2CH(OH)SO_3^- \quad \text{(slow)} \qquad (3a)$$

$$CHOCHO + HSO_3^- \underset{k''_{-1}}{\overset{k''_1}{\rightleftharpoons}} CHOCH(OH)SO_3^- \quad \text{(slow)} \qquad (3b)$$

$$CH(OH)_2CHO + SO_3^{2-} \underset{k'_{-2}}{\overset{k'_2}{\rightleftharpoons}} CH(OH)_2CH(O^-)SO_3^- \quad \text{(slow)} \qquad (4a)$$

$$CHOCHO + SO_3^{2-} \underset{k''_{-2}}{\overset{k''_2}{\rightleftharpoons}} CHOCH(O^-)SO_3^- \quad \text{(slow)} \qquad (4b)$$

$$CH(OH)_2CH(OH)SO_3^- \overset{K'_{a2,GMBS}}{\rightleftharpoons} H^+ + CH(OH)_2CH(O^-)SO_3^- \quad \text{(fast)} \qquad (5a)$$

$$CHOCH(OH)SO_3^- \overset{K''_{a2,GMBS}}{\rightleftharpoons} H^+ + CHOCH(O^-)SO_3^- \quad \text{(fast)} \qquad (5b)$$

Although glyoxal is assumed to be present primarily as the dihydrate, $(CH(OH)_2)_2$, values of K_{D1} and K_{D2} are not well-known. Wasa and Musha[11] obtained a value of the product, $K_{D1}K_{D2} = [CHOCHO]/[(CH(OH)_2)_2]$, as 4.6×10^{-6} at 25 °C using polarography and 2.52 M glyoxal solutions. They admitted, however, that their results may have been affected by the presence of polymers. Such interference seems likely in view of what is now known about other β-hydroxyaldehydes such as hydroxyacetaldehyde ($CH_2(OH)CHO$). Proton NMR studies have revealed that at least two dimer forms of hydroxyacetaldehyde

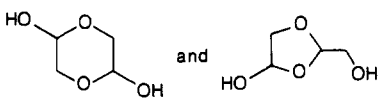

are present in 0.1 M aldehyde-in-D_2O solutions at concentrations of 9 and 17% respectively at 35 °C.[12,13]

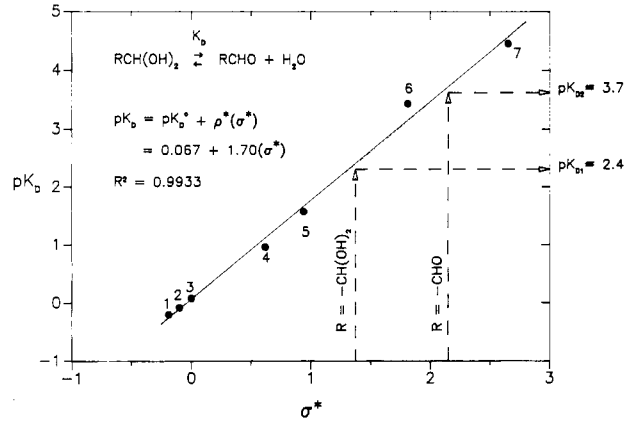

Figure 4. Linear free-energy relationship between pK_D and σ^*. Key: 1, $(CH_3)_2CHCHO$ (ref 14); 2, CH_3CH_2CHO (ref 15); 3, CH_3CHO (ref 15); 4, $CH_2(OH)CHO$ (ref 16); 5, $ClCH_2CHO$ (ref 17); 6, CH_3COCHO (ref 11); 7, Cl_3CCHO (ref 18). Formaldehyde (σ^*_{HCHO} = 0.49, $pK_{D,HCHO}$ = 3.26 (ref 17)) lies well above the least-squares regression line and was not included.

Estimates of K_{D1} and K_{D2} can be calculated from linear free energy relationships, such as the Taft equation

$$pK_D = pK_D^0 + \rho^*\sigma^* \qquad (6)$$

where K_D^0 is the dehydration constant for acetaldehyde, σ^* are the Taft polar substituent constants for group R in $RCH(OH)_2$, and ρ^* is the characteristic slope for the reaction. Using literature values of K_D[14-18] and σ^*[19] for carbonyl compounds with a single α-hydrogen, the correlation in Figure 4 was developed. Estimates of K_{D1} and K_{D2} are 2.0×10^{-4} and 4.2×10^{-3}, respectively, and the product, $K_{D1}K_{D2}$, is more than an order of magnitude smaller than Wasa and Musha's experimental value. The correlation estimates support the assumption that $(CH(OH)_2)_2$ is the predominant glyoxal species. Further supporting evidence is the absence of the characteristic carbonyl $n \rightarrow \pi^*$ absorption band near 280 nm[20] in glyoxal's absorbance spectrum.

The acid-dissociation constants, K'_{a2} and K''_{a2}, for GMBS are also not well-known. However, pK_{a2} values for other aldehyde–S(IV) addition compounds are typically in the range of 9–12[5b] so that, under our pH conditions, the adducts are expected to exist primarily as the singly protonated species.

Under conditions which lie far to the left of equilibrium, eq 1–5 give the following rate expression for GMBS formation

$$v = \frac{d[GMBS]}{dt} = (k'_1[CH(OH)_2CHO] + k''_1[CHOCHO])[HSO_3^-] + (k'_2[CH(OH)_2CHO] + k''_2[CHOCHO])[SO_3^{2-}] \qquad (7)$$

which may be further simplified as

$$v = \{(k'_1\beta_1 + k''_1\beta_2)\alpha_1 + (k'_2\beta_1 + k''_2\beta_2)\alpha_2\}[S(IV)][C_2H_2O_2] \qquad (8)$$

(11) Wasa, T.; Musha, S. *Bull. Univ. Osaka Prefect Ser. A* **1970**, *19*, 169–80.

(12) Collins, G. C. S.; George, W. O. *J. Chem. Soc. B* **1971**, 1352–55.

(13) Kobayashi, Y.; Takahashi, H. *Spectrochim. Acta, Part A* **1979**, *35A*, 307–14.

(14) Hine, J.; Houston, J. G.; Jensen, J. H. *J. Org. Chem.* **1965**, *30*, 1184–88.

(15) Buschmann, H. J.; Füldner, H. H.; Knoche, W. *Ber. Bunsen-Ges. Phys. Chem.* **1980**, *84*, 41–44.

(16) Sorensen, P. E. *Acta Chem. Scand.* **1972**, *26*, 3357–65.

(17) Bell, R. P. In *Advances in Physical Organic Chemistry*; Gold, V., Ed.; Academic: London, 1966; Vol. 4, pp 1–29.

(18) Gruen, L. C.; McTigue, P. T. *J. Chem. Soc.* **1963**, 5224–29.

(19) Perrin, D. D.; Dempsey, B.; Serjeant, E. P. *pKa Prediction for Organic Acids and Bases*; Chapman and Hall: London, 1981; pp 37–8, 109–25.

(20) Rao, C. N. R. *Ultra-Violet and Visible Spectroscopy*, 2nd ed.; Butterworth: London, 1967; p 15.

where

$$\beta_1 = \frac{[CH(OH)_2CHO]}{[C_2H_2O_2]} = \frac{K_{D1}}{1 + K_{D1} + K_{D1}K_{D2}} \quad (9)$$

$$\beta_2 = \frac{[CHOCHO]}{[C_2H_2O_2]} = \frac{K_{D1}K_{D2}}{1 + K_{D1} + K_{D1}K_{D2}} \quad (10)$$

$$[S(IV)] = [H_2O{\cdot}SO_2] + [HSO_3^-] + [SO_3^{2-}] \quad (11a)$$

$$[C_2H_2O_2] = [CHOCHO] + [CHOCH(OH)_2] + [(CH(OH)_2)_2] \quad (11b)$$

$$\alpha_1 = \frac{[HSO_3^-]}{[S(IV)]} = \frac{K_{a1}\{H^+\}}{\{H^+\}^2 + K_{a1}\{H^+\} + K_{a1}K_{a2}} \quad (12)$$

$$\alpha_2 = \frac{[SO_3^{2-}]}{[S(IV)]} = \frac{K_{a1}K_{a2}}{\{H^+\}^2 + K_{a1}\{H^+\} + K_{a1}K_{a2}} \quad (13)$$

When a large excess of glyoxal is present, $[C_2H_2O_2] \approx [C_2H_2O_2]_t$ and the observed rate constant becomes

$$k_{obsd} = \{(k'_1\beta_1 + k''_1\beta_2)\alpha_1 + (k'_2\beta_1 + k''_2\beta_2)\alpha_2\}[C_2H_2O_2]_t \quad (14)$$

In aqueous solutions alone it is not possible to determine the intrinsic rate constants, k'_1, k''_1, k'_2, and k''_2. Consequently the following substitution in eq 14 will be made to simplify the notation

$$k_{1,app} = k'_1\beta_1 + k''_1\beta_2 \quad (15a)$$

$$k_{2,app} = k'_2\beta_1 + k''_2\beta_2 \quad (15b)$$

giving

$$k_{obsd} = (k_{1,app}\alpha_1 + k_{2,app}\alpha_2)[C_2H_2O_2]_t \quad (16)$$

Dividing k_{obsd} by $\alpha_1[C_2H_2O_2]_t$ gives

$$\frac{k_{obsd}}{\alpha_1[C_2H_2O_2]_t} = k_{1,app} + k_{2,app}(\alpha_2/\alpha_1) \quad (17)$$

and an estimate of $k_{1,app} \approx 0.15$ M^{-1} s^{-1} therefore can be obtained from the intercept of Figure 2. Since the magnitudes of K_{a1} and K_{a2} (25 °C, μ = 0) are 1.45×10^{-2} M[21] and 6.31×10^{-8} M,[22] respectively, the approximations that $K_{a1}\{H^+\} \gg \{H^+\}^2$ and $K_{a1}\{H^+\} \gg K_{a1}K_{a2}$ can be made in the pH region of 2.5–3.2. Equation 16 then can be approximated as

$$k_{obsd} \approx \{k_{1,app} + k_{2,app}K_{a2}/\{H^+\}\}[C_2H_2O_2]_t \quad (18)$$

An estimate of $k_{2,app} \approx 2.21 \times 10^3$ M^{-1} s^{-1} was obtained by plotting $k_{obsd}/[C_2H_2O_2]_t$ vs $1/\{H^+\}$ as shown in Figure 3 and dividing the slope by K_{a2}.

Refined estimates of $k_{1,app}$ and $k_{2,app}$ were obtained by fitting all of the data in Table I to eq 16 with a nonlinear least-squares regression routine.[23a] Our rough estimates of the rate constants were supplied as initial guesses to the fitting program. The values of K_{a1} and K_{a2} were held fixed in the regression analysis but were corrected for an ionic strength of 0.2 M. The corrected acidity constants were ${}^cK_{a1} = K_{a1}\gamma_{H_2O{\cdot}SO_2}/\gamma_{HSO_3^-} = 1.99 \times 10^{-2}$ M and ${}^cK_{a2} = K_{a2}\gamma_{HSO_3^-}/\gamma_{SO_3^{2-}} = 1.63 \times 10^{-7}$ M, where K_{a1} and K_{a2} refer to acidity constants at infinite dilution. Activity coefficients, γ, were computed with the Davies equation[24]

$$\log \gamma = -Az^2\left(\frac{\mu^{1/2}}{\mu^{1/2} + 1} + 0.2\mu\right) \quad (19)$$

where $A = 0.509$ (for water at 25 °C), z is the ionic charge, and μ is the ionic strength. From the regression analysis, the refined estimates are $k_{1,app} = 0.130$ (± 0.014) M^{-1} s^{-1} and $k_{2,app} = 2.08$ (± 0.05) $\times 10^3$ M^{-1} s^{-1}. A comparison of observed and calculated pseudo-first-order rate constants (based on the fitted values of $k_{1,app}$ and $k_{2,app}$) is presented in Table I.

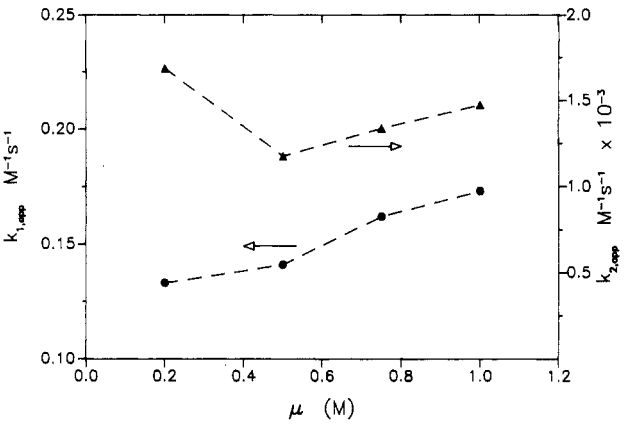

Figure 5. Ionic strength dependence of $k_{1,app}$ and $k_{2,app}$ (25 °C).

The ionic strength dependence of $k_{1,app}$ and $k_{2,app}$ between μ = 0.2 and 1.0 M was expected to be slight since both constants correspond to the addition of an anion or dianion with a neutral molecule. This assumption was experimentally tested and, as Figure 5 demonstrates, $k_{1,app}$ and $k_{2,app}$ are nearly independent of μ between μ = 0.2 and 1.0 M.

Although the possibility of general acid catalysis by the buffers used herein was not tested, such catalysis has not been found for the addition of bisulfite and sulfite with other aldehydes.[3,4] In addition, an absence of general acid or base catalysis is a well-known characteristic for the reaction of strong nucleophilic reagents with the carbonyl group.[25] Buffer effects in the glyoxal–S(IV) system are therefore expected to be minimal over the pH range used here.

Adduct Dissociation Kinetics. By monitoring the dissociation of GDBS and GMBS in the presence of I_2, the reaction proceeded irreversibly as follows:

$$GDBS \xrightarrow{k_{-1,obsd}} GMBS + S(IV) \quad (slow) \quad (20)$$

$$GMBS \xrightarrow{k_{-2,obsd}} glyoxal + S(IV) \quad (slow) \quad (21)$$

$$I_2 + S(IV) \rightarrow 2I^- + S(VI) \quad (fast) \quad (22)$$

and hence the kinetic analysis was greatly simplified. At constant pH, the corresponding rate equation is

$$v = -d[I_3^-]/dt = k_{-1,obsd}[GDBS]_t + k_{-2,obsd}[GMBS]_t \quad (23)$$

where

$$[GMBS]_t = [CH(OH)_2CH(OH)SO_3^-] + [CH(OH)_2CH(O^-)SO_3^-] + [CHOCH(OH)SO_3^-] + [CHOCH(O^-)SO_3^-] \quad (24a)$$

$$[GDBS]_t = [(CH(OH)SO_3^-)_2] + [CH(OH)SO_3^-CH(O^-)SO_3^-] \quad (24b)$$

and is subject to the initial conditions

$$[GDBS]_0 = C_0; \quad [GMBS]_0 = 0; \quad [S(IV)]_0 = 0$$

Equation 23 is readily integrable and the solution satisfying the initial conditions can be written in the form

$$\frac{A - A_\infty}{A_0 - A_\infty} = \frac{1}{2}\left\{\left[1 + \frac{k_{-2,obsd}}{(k_{-2,obsd} - k_{-1,obsd})}\right]e^{-(k_{-1,obsd}t)} - \left[\frac{k_{-1,obsd}}{(k_{-2,obsd} - k_{-1,obsd})}\right]e^{-(k_{-2,obsd}t)}\right\} \quad (25)$$

The two first-order rate constants were fit to each data set with

(21) Deveze, D.; Rumpf, P. *C.R. Acad. Sci. Paris* **1964**, *258*, 6135–38.
(22) Hayon, E.; Treinin, A.; Wilf, J. *J. Am. Chem. Soc.* **1972**, *94*, 47–57.
(23) (a) "STAT/LIBRARY FORTRAN Subroutines for Statistical Analysis On a Personal Computer"; IMSL User Manual, 1984. (b) "MATH/LIBRARY Problem-Solving Software System for Mathematical FORTRAN Programming"; IMSL User Manual, 1984.
(24) Stumm, W.; Morgan, J. J. *Aquatic Chemistry*, 2nd ed.; Wiley-Interscience: New York, 1981; p 135.
(25) Jencks, W. P. *Prog. Phys. Chem.* **1964**, *2*, 63–118.

TABLE II: Kinetic Data for the Dissociation of Glyoxal Monobisulfite and Glyoxal Dibisulfite Addition Compounds

pH	$k_{1,obsd}$ ($\pm\sigma$), s^{-1}	$k_{2,obsd}$ ($\pm\sigma$), s^{-1}
1.26	1.24 (0.03) × 10^{-5}	4.01 (0.01) × 10^{-6}
1.80	1.49 (0.13) × 10^{-5}	4.22 (0.04) × 10^{-6}
3.00	8.37 (0.37) × 10^{-5}	1.85 (0.21) × 10^{-5}
3.88	5.65 (0.18) × 10^{-4}	9.27 (0.12) × 10^{-5}
4.53	2.16 (0.16) × 10^{-3}	4.25 (0.10) × 10^{-4}
4.87	5.85 (0.23) × 10^{-3}	9.08 (0.03) × 10^{-4}
5.09	1.05 (0.07) × 10^{-2}	1.38 (0.03) × 10^{-3}
5.92	7.58 (0.30) × 10^{-2}	8.22 (0.11) × 10^{-2}
6.49	0.278 (0.004)	3.00 (0.12) × 10^{-2}
6.99	0.858 (0.001)	9.53 (0.35) × 10^{-2}

a nonlinear least-squares regression route.[23a] Results of this analysis as a function of pH are tabulated in Table II. Plots of log $k_{-1,obsd}$ and log $k_{-2,obsd}$ vs pH have slopes of approximately unity above pH 4 and are nearly pH-independent near pH 1 as shown in Figure 6. This pH dependence was also observed for the dissociation of benzaldehyde- and methylglyoxal–S(IV) addition compounds[5,26] and can be explained with the following mechanism and eq 5a,b

$$(CH(OH)SO_3^-)_2 \xrightarrow{k_{-3}} CHOCH(OH)SO_3^- + HSO_3^- \quad \text{(slow)} \quad (26)$$

$$CH(OH)SO_3^-CH(O^-)SO_3^- \xrightarrow{k_{-4}} CH(OH)SO_3^-CHO + SO_3^{2-} \quad \text{(slow)} \quad (27)$$

$$CH(OH)_2CH(OH)SO_3^- \xrightarrow{k'_{-1}} CH(OH)_2CHO + HSO_3^- \quad \text{(slow)} \quad (28a)$$

$$CHOCH(OH)SO_3^- \xrightarrow{k''_{-1}} CHOCHO + HSO_3^- \quad \text{(slow)} \quad (28b)$$

$$CH(OH)_2CH(O^-)SO_3^- \xrightarrow{k'_{-2}} CH(OH)_2CHO + SO_3^{2-} \quad \text{(slow)} \quad (29a)$$

$$CHOCH(O^-)SO_3^- \xrightarrow{k''_{-2}} CHOCHO + SO_3^{2-} \quad \text{(slow)} \quad (29b)$$

$$CH(OH)_2CH(OH)SO_3^- \overset{K_{D3}}{\rightleftharpoons} CHOCH(OH)SO_3^- + H_2O \quad \text{(fast)} \quad (30)$$

$$(CH(OH)SO_3^-)_2 \overset{K_{a3,GDBS}}{\rightleftharpoons} H^+ + CH(OH)SO_3^-CH(O^-)SO_3^- \quad \text{(fast)} \quad (31)$$

The rate expression governing the rate of release of S(IV)

$$\nu = k'_{-1}[CH(OH)_2CH(OH)SO_3^-] + k''_{-1}[CHOCH(OH)SO_3^-] + k'_{-2}[CH(OH)_2CH(O^-)SO_3^-] + k''_{-2}[CHOCH(O^-)SO_3^-] + k_{-3}[(CH(OH)SO_3^-)_2] + k_{-4}[CH(OH)SO_3^-CH(O^-)SO_3^-] \quad (32)$$

can be rewritten in terms of $[GMBS]_t$ and $[GDBS]_t$ to give

$$\nu = \left\{k'_{-1} + k''_{-1}K_{D3} + \frac{(k'_{-2}K'_{a2,GMBS} + k''_{-2}K''_{a2,GMBS}K_{D3})}{\{H^+\}}\right\}[GMBS]_t + \left\{k_{-3} + \frac{k_{-4}K_{a3,GDBS}}{\{H^+\}}\right\}[GDBS]_t \quad (33)$$

In deriving eq 33, it was assumed that $[CH(OH)_2CH(OH)SO_3^-] \approx [GMBS]_t$ and $[(CH(OH)SO_3^-)_2] \approx [GDBS]_t$. Although the former assumption depends on the magnitude of K_{D3}, an unknown, GMBS is likely to have a relatively large σ^* value and hence be predominantly hydrated. The proposed mechanism leads to the following representations for the observed rate constants

$$k_{-1,obsd} = k_{-3} + (k_{-4}K_{a3,GDBS})/\{H^+\} \quad (34a)$$

$$k_{-2,obsd} = (k'_{-1} + k''_{-1}K_{D3}) + (k'_{-2}K'_{a2,GMBS} + k''_{-2}K''_{a2,GMBS}K_{D3})/\{H^+\} \quad (34b)$$

and these are consistent with the data in Figure 6. Plots of $k_{-1,obsd}$ and $k_{-2,obsd}$ vs $1/\{H^+\}$ over the entire pH range were linear ($R^2 > 0.9999$) and the slopes were used to estimate the apparent constants $k'_{-2}K'_{a2} + k''_{-2}K''_{a2,GMBS}K_{D3}$ and $k_{-4}K_{a3,GDBS}$, given in Table III. The values of k_{-3} and $k'_{-1} + k''_{-1}K''_{a2,GMBS}$ in Table III were obtained from the intercepts, using only the data below pH 4.

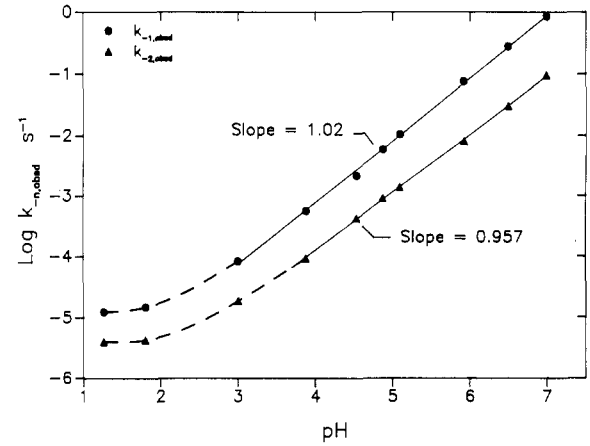

Figure 6. Dissociation rate constants for GDBS ($k_{-1,obsd}$) and GMBS ($k_{-2,obsd}$) as a function of pH. Solid lines are linear least-squares regression fits to the data in Table II.

TABLE III: Dissociation Rate Constant Estimates at 25 °C, μ = 0.2 M

constant term	value
$k'_{-1} + k''_{-1}K_{D3}$	4.62 × 10^{-6} s^{-1}
$k'_{-2}K'_{a2} + k''_{-2}K''_{a2,GMBS}K_{D3}$	9.74 × 10^{-9} s^{-1} M
k_{-3}	1.07 × 10^{-5} s^{-1}
$k_{-4}K_{a3,GDBS}$	8.80 × 10^{-8} s^{-1} M

Adduct Stability Constants. The predominant adduct, S(IV), and glyoxal species remain the same between pH 3 to 5 and hence measurements of $K_{1,app}$ and $K_{2,app}$ where

$$K_{1,app} = \frac{[GMBS]}{[C_2H_2O_2][S(IV)]} \quad (35a)$$

$$K_{2,app} = \frac{[GDBS]}{[GMBS][S(IV)]} \quad (35b)$$

should be pH independent over this pH range and approximately given by

$$K_{1,app} \approx {}^cK_1 = \frac{[CH(OH)_2CH(OH)SO_3^-]}{[(CH(OH)_2)_2][HSO_3^-]} \quad (36a)$$

$$K_{2,app} \approx {}^cK_2 = \frac{[(CH(OH)SO_3^-)_2]}{[CH(OH)_2CH(OH)SO_3^-][HSO_3^-]} \quad (36b)$$

Furthermore, when $[C_2H_2O_2]_t$ is sufficiently greater than $[S(IV)]_t$, [GDBS] is negligible and hence,

$${}^cK_1 \approx \frac{([S(IV)]_t - [S(IV)]_{eq})}{\{[C_2H_2O_2]_t - ([S(IV)]_t - [S(IV)]_{eq})\}[S(IV)]_{eq}} \quad (37)$$

With a tenfold excess of glyoxal, measurements of $[S(IV)]_{eq}$ at

(26) Stewart, T. D.; Donnally, L. H. *J. Am. Chem. Soc.* **1932**, *54*, 2333–40.

TABLE IV: S(IV) Concentrations in Equilibrated Disodium Glyoxal Dibisulfite Solutions at 25 °C, μ = 0.2 M, pH 3.4–3.6

$10^5[(NaCH(OH)SO_3)_2]_t$, M	$10^5[S(IV)]_{eq,measd}$, M	$10^5[S(IV)]_{eq,calcd}$,[a] M
1.0	1.59	1.53
2.0	2.60	2.58
3.0	3.37	3.42
4.0	4.18	4.14
5.0	4.70	4.77
6.0	5.33	5.34
7.0	5.89	5.87
8.0	6.39	6.36

[a] Based on ${}^cK_1 = 3.57 \times 10^4$ M^{-1} and ${}^cK_2 = 1.45 \times 10^4$ M^{-1}.

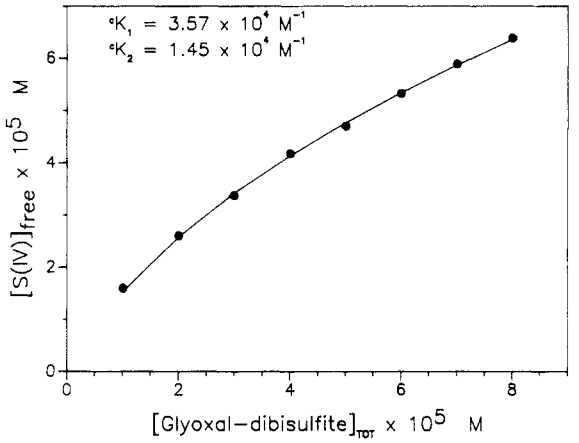

Figure 7. Measured free [S(IV)] at equilibrium as a function of total $[Na_2(CH(OH)SO_3)_2]$. Conditions: T = 25 °C, μ = 0.2 M, pH 3.6. Solid line represents nonlinear least-squares regression fit of ${}^cK_1$ and ${}^cK_2$ to the data in Table IV using eq 39.

three different pH's were used in eq 37 to obtain an average ${}^cK_1 = 2.81 \times 10^4$ M^{-1} at 25 °C and μ = 0.2 M.

In solutions of the disodium glyoxal dibisulfite salt (i.e., $[S(IV)]_t = 2[C_2H_2O_2]_t$), both GMBS and GDBS species may be present. Mass balance and mass action relationships can be shown to yield the following expression for ${}^cK_2$ under these conditions:

$$ {}^cK_2 = \frac{{}^cK_1[S(IV)]_{eq}^2 + [S(IV)]_{eq}(1 - {}^cK_1[C_2H_2O_2]_t) - 2[C_2H_2O_2]_t}{-{}^cK_1[S(IV)]_{eq}^3} \quad (38) $$

The concentration of free S(IV) at equilibrium is therefore a root of the cubic equation:

$$ {}^cK_1{}^cK_2[S(IV)]_{eq}^3 + {}^cK_1[S(IV)]_{eq}^2 + (1 - {}^cK_1[C_2H_2O_2]_t)[S(IV)]_{eq} - 2[C_2H_2O_2]_t = 0 \quad (39) $$

The magnitudes of ${}^cK_1$ and ${}^cK_2$ were obtained by fitting the data in Table IV to eq 39. Since it was not possible to write an analytic expression for $[S(IV)]_{eq}$ in terms of ${}^cK_1$, ${}^cK_2$, and $[C_2H_2O_2]_t$, the nonlinear least-squares regression routine had to be coupled to an algorithm which could solve for the zeroes of eq 39.[23a,b] Estimates for ${}^cK_1$ and ${}^cK_2$ at 25 °C and μ = 0.2 M were 3.57×10^4 and 1.45×10^4 M^{-1}, respectively. Measured free S(IV) concentrations are compared with the calculated function in Figure 7.

Formation constants at infinite dilution, ${}^aK$, can be computed by using eq 40a,b and the Davies equation to estimate the activity coefficients of the ionic species.

$$ {}^aK_1 = {}^cK_1\left\{\frac{\gamma_{GMBS^-}}{\gamma_{(CH(OH)_2)_2}\gamma_{HSO_3^-}}\right\} \quad (40a) $$

$$ {}^aK_2 = {}^cK_2\left\{\frac{\gamma_{GDBS^{2-}}}{\gamma_{GMBS^-}\gamma_{HSO_3^-}}\right\} \quad (40b) $$

TABLE V: Apparent Stability Constants for Glyoxal Mono- and Dibisulfite Addition Compounds

method	T, °C	μ, M	$10^{-4c}K_1$ ($\pm\sigma$), M^{-1}	$10^{-4c}K_2$ ($\pm\sigma$), M^{-1}
A	25	0.2	2.81	N/A
B	25	0.2	2.81 (0.14)	N/A
C	25	0.2	3.57 (0.42)	1.45 (0.15)
C	25	1.0	4.66 (0.89)	2.44 (0.34)
C	30	0.2	2.95 (0.46)	1.08 (0.16)
C	35	0.2	2.44 (0.51)	0.87 (0.22)

[a] Method A: ${}^cK_1$ calculated from forward and reverse rate constants. Method B: $[S(IV)]_{eq}$ measured with a tenfold excess of glyoxal. Method C: $[S(IV)]_{eq}$ measured in dissolved $Na_2(CH(OH)SO_3)_2$ solutions.

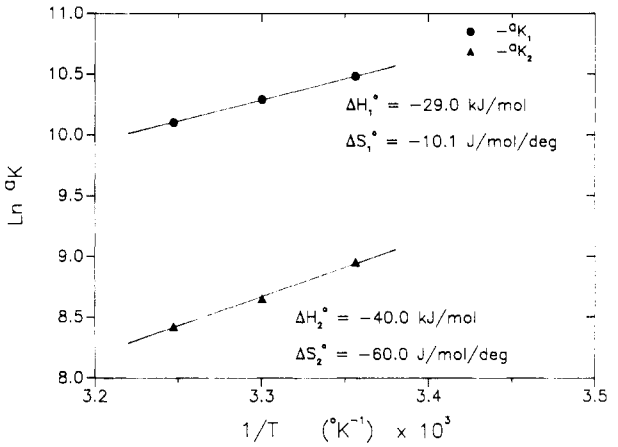

Figure 8. Temperature dependence of GMBS and GDBS stability constants (${}^aK_1$ and ${}^aK_2$, respectively). Stability constants in Table V have been corrected from μ = 0.2 to μ = 0 with eq 19.

If $\gamma_{(CH(OH)_2)_2} \approx 1$, use of the Davies equation in (40a) implies that ${}^cK_1$ should be relatively insensitive to ionic strength and hence ${}^aK_1 \approx 3.57 \times 10^4$ M^{-1}. A separate determination of ${}^cK_1$ (see Table V) at μ = 1.0 M suggests that this hypothesis is approximately correct since ${}^cK_1$ increased by only 30% over a fivefold increase in μ. Based on eq 40b and our estimate of ${}^cK_2$ at μ = 0.2 M, ${}^aK_2 = 7.70 \times 10^3$ M^{-1} at 25 °C. Standard enthalpy ($\Delta H°_1 = -29.0$ and $\Delta H°_2 = -40.0$ kJ/mol) and entropy ($\Delta S°_1 = -10.1$ and $\Delta S°_2 = -60.0$ J/(mol/deg)) changes were calculated from the results of temperature studies and the van't Hoff plot shown in Figure 8.

Discussion

The mechanism outlined in eq 1–5 is similar to those we have proposed for the formation of other aldehyde–S(IV) adducts[3–5] over the same pH range (0.7–3.2). Outside this pH domain, however, other rate-determining steps are possible and have been observed with other aldehydes. Above pH 4.0, for example, dehydration of the methylglyoxal diol species becomes the rate-limiting step for adduct formation[5] and similar predictions have been made for formaldehyde.[27] We are unable to make the analogous prediction for GMBS formation since reliable values of the necessary dehydration rate constants are not available. Below pH 0.7 other adduct formation pathways may be important. Specific acid catalysis was observed at very low pH for both benzaldehyde and methylglyoxal. This catalysis was attributed to the protonation of the carbonyl carbon which thereby provides a more electrophilic site for attack by bisulfite.

The magnitudes of $k_{1,app}$ and $k_{2,app}$ reported in this study reflect the large difference in reactivity between HSO_3^- and SO_3^{2-} with aldehydes. The ratio of $k_{2,app}/k_{1,app}$ for GMBS is 1.6×10^4, which is slightly lower than the corresponding ratios of other aldehydes (CH_3COCHO, 1.14×10^5; C_6H_5CHO, 3.02×10^4; HCHO, 3.14×10^4). Our lower value for glyoxal may be due to the fact that the rate constants were not intrinsic. Other investigators have

(27) Olson, T. M.; Hoffmann, M. R. *Atmos. Environ.* **1986**, *11*, 2277–78.

TABLE VI: Potential Aqueous Glyoxal–S(IV) Adduct Concentrations (μM) in an Open Atmosphere (P_{SO_2} = 20 ppbv, P_{CHOCHO} = 0.1 ppbv, T = 25 °C)

pH	[GMBS]	[GDBS]	$[S(IV)]_t$[a]	$[C_2H_2O_2]_t$[b]	$[C_2H_2O_2]_t/[(CH(OH)_2)_2]$	$[S(IV)]_t/[S(IV)]_{free}$
3	0.308	0.0009	0.70	30.3	1.01	1.79
4	3.08	0.087	6.93	33.2	1.11	1.89
5	30.9	8.67	84.7	69.5	2.32	2.32
6	308	867	2430	1200	40.0	6.26

[a] $[S(IV)]_t = [H_2O{\cdot}SO_2] + [HSO_3^-] + [SO_3^{2-}] + [GMBS]_t + 2[GDBS]_t$. [b] $[C_2H_2O_2]_t = [(CH(OH)_2)_2] + [GMBS] + [GDBS]$.

also found SO_3^{2-} to be the strongest nucleophile among S(IV) species in reactions with a wide variety of inorganic and organic substrates.[28,29] Besides the expected difference in nucleophilicity of SO_3^{2-} and HSO_3^-, the greater reactivity of sulfite may involve structural differences in the transition-state complexes. In our previous studies with formaldehyde, benzaldehyde, and methylglyoxal, we proposed that bisulfite addition requires the formation of a cyclic activated complex, whereas sulfite addition does not. Measured activation parameters in these studies supported this hypothesis since a much larger activation entropy was found for HSO_3^- addition than the ΔS^* for SO_3^{2-}.

Above pH 3, the decomposition of $RCH(O^-)SO_3^-$ species governs the dissociation kinetics of GMBS and GDBS. This behavior reflects the large difference in rate constants for the release of HSO_3^- and SO_3^{2-}. A minimum value of the ratio, $k_{-4}/k_{-3} > 10^6$, can be estimated, for example, using the data in Table III and assuming a conservative limit of $K_{a3,GDBS} < 10^{-9}$. The more rapid dissociation of $RCH(O^-)SO_3^-$ species may be attributed to the inductive effect of its electron-donating group, O^- group. The release of bisulfite would be less favorable since the hydroxy group withdraws electrons from the carbon center.

Applying the principle of microscopic reversibility, a third independent estimate of the stability constant for GMBS is $^cK_1 = k_{1,app}/(k'_{-1} + k''_{-1}K_{D3}) = 2.81 \times 10^4$ M^{-1} (25 °C, μ = 0.2 M). This value of $^cK_1$ agrees closely with the one determined by method B but is slightly less than the stability constant obtained by method C (see Table V). Since the standard error associated with the method C value of $^cK_1$ is also quite large, we believe the more reliable estimate of $^cK_1$ is 2.81×10^4 M^{-1}.

Reasonable agreement was also found between our value of the second association constant, $^aK_2 = 7.70 \times 10^3$ M^{-1} (25 °C, μ = 0) and Salomaa's data.[9] The apparent constant cited by Salomaa at pH 7.3 (equivalent to $K_{2,app}$ defined in eq 35b) gives a value of $^cK_2 = 8.61 \times 10^3$ M^{-1} at 20 °C. Temperature corrections based on our reported values of ΔH°_2 and ΔS°_2 increase $^aK_2$ to 1.00×10^4 M^{-1} at 20 °C; however, direct comparison of this number with Salomaa's is still not exact since the ionic strength in his study is not known.

In Figure 9 a linear free-energy plot relates S(IV)–aldehyde adduct stability constants (now expressed in terms of the *unhydrated* aldehyde concentration) and Taft polar substituent constants. In order to include the formation constant for glyoxal monobisulfite in this correlation, values of $K_{D1} \approx 2.0 \times 10^{-4}$ and $K_{D2} \approx 4.2 \times 10^{-3}$ were assumed (vide supra). The stability constant for GDBS was not compared in the correlation since the σ^* parameter for the substituent, $-CH(OH)SO_3^-$, has not been established. Taft correlations for K_D (Figure 4) and K_1 (Figure 9) are strikingly similar in that aliphatic carbonyl substrates with a single α-hydrogen are linear in σ^*. Formaldehyde, which has two α-hydrogen atoms, forms more stable adducts ($CH_2(OH)_2$ and $CH_2(OH)SO_3^-$) than the lines in Figures 4 and 9 would predict. The enhanced stability observed when methyl groups are replaced by hydrogen atoms may be due to an increase in hydrogen bonding with the solvent water and the subsequent increased polarization of the carbonyl group.

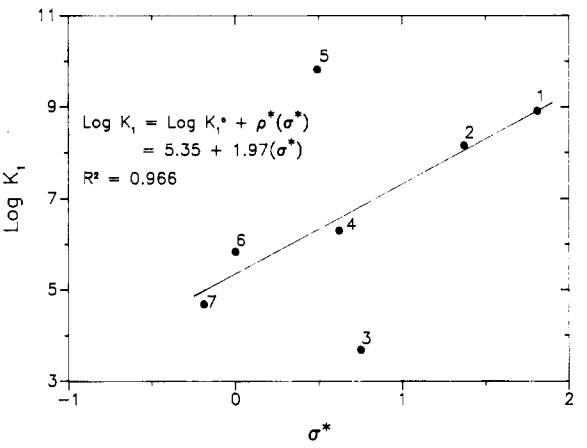

Figure 9. Linear free-energy plot of aldehyde–S(IV) stability constants ($K_1 = [RCH(OH)SO_3^-]/([RCHO][HSO_3^-])$) vs σ^* at 25 °C. Key: 1, CH_3COCHO (ref 5a); 2, $CH(OH)_2CHO$ (this work); 3, C_6H_5CHO (ref 4); 4, $CH_2(OH)CHO$ (ref 5b); 5, HCHO (ref 5b); 6, $(CH_3)_2CHCHO$ (ref 31); 7, CH_3CHO (ref 30). The solid line was calculated from a least-squares fit of data for points 1, 2, 4, 6, and 7 only.

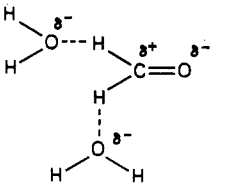

Similar hydrogen-bonding arguments have been invoked to explain Taft correlations for acidity constants of primary, secondary, and tertiary amines.[19] Benzaldehyde–water and –bisulfite addition compounds are substantially less stable than the lines in Figures 4 and 9 would predict. The lack of correlation in this case may be due to resonance stabilization of free benzaldehyde and/or to steric hindrance by the phenyl group.

Conclusions for Atmospheric Systems. With the above thermodynamic data it is now possible to examine the importance of glyoxal–S(IV) adducts as reservoirs for S(IV) and glyoxal. Maximum concentrations of aqueous GMBS and GDBS which could form in a polluted open atmosphere were calculated with the following mass balances and Henry's law relationships:

$$[S(IV)]_t = [H_2O{\cdot}SO_2] + [HSO_3^-] + [SO_3^{2-}] + [GMBS]_t + 2[GDBS]_t \quad (41a)$$

$$[C_2H_2O_2]_t = [(CH(OH)_2)_2] + [GMBS]_t + [GDBS]_t \quad (41b)$$

$$[H_2O{\cdot}SO_2] = P_{SO_2}H^*_{SO_2} \quad (42a)$$

$$[HSO_3^-] = P_{SO_2}H^*_{SO_2}K_{a1}/\{H^+\} \quad (42b)$$

$$[SO_3^{2-}] = P_{SO_2}H^*_{SO_2}K_{a1}K_{a2}/\{H^+\} \quad (42c)$$

$$[(CH(OH)_2)_2] = P_{CHOCHO}H^*_{CHOCHO} \quad (42d)$$

$$[GMBS]_t \simeq [CH(OH)_2CH(OH)SO_3^-] = {}^cK_1P_{CHOCHO}H^*_{CHOCHO}P_{SO_2}H^*_{SO_2}K_{a1}/\{H^+\} \quad (42e)$$

(28) Schroeter, L. C. *Sulfur Dioxide, Applications in Foods, Beverages, and Pharmaceuticals*; Pergamon: New York, 1966; pp 119–20.
(29) Edwards, J. O. *Inorganic Reaction Mechanisms*; Benjamin: New York, 1965; pp 54–56.
(30) Deister, U.; Neeb, R.; Helas, G.; Warneck, P. *J. Phys. Chem.* **1986**, *90*, 3213–17.
(31) Green, L. R.; Hine, J. *J. Org. Chem.* **1974**, *39*, 3896–901.

$$[\mathrm{GDBS}]_t \simeq [(\mathrm{CH(OH)SO_3^-})_2]$$

$$= {}^cK_1{}^cK_2 P_{\mathrm{CHOCHO}} H^*_{\mathrm{CHOCHO}} [P_{\mathrm{SO_2}} H^*_{\mathrm{SO_2}} K_{a1} / \{\mathrm{H^+}\}]^2 \quad (42f)$$

where P_{CHOCHO} and $P_{\mathrm{SO_2}}$ are the partial pressures of gas-phase species, and H^*_{CHOCHO} and $H^*_{\mathrm{SO_2}}$ are apparent Henry's law constants.

Since ambient SO_2 levels in polluted atmospheres generally range from 0 to 50 ppbv,[1] a typical SO_2 partial pressure of 20 ppbv was selected. Typical gas-phase concentrations of glyoxal have not been established. However, a value of 0.1 ppbv leads to an aqueous concentration of 30 μM glyoxal if the apparent Henry's law constant is approximately 3×10^5 M atm^{-1}.[32] Although glyoxal photolyzes quite rapidly in the gas phase, with predicted atmospheric lifetimes of a few hours,[33] the above aqueous glyoxal concentration is comparable to those reported in mist and fogwater.[8]

Adduct concentrations and S(IV) and glyoxal enrichment factors (i.e., $[\mathrm{S(IV)}]_t/[\mathrm{S(IV)}]_{\mathrm{free}}$ and $[\mathrm{C_2H_2O_2}]_t/[(\mathrm{CH(OH)_2})_2]$) corresponding to the above conditions are tabulated in Table VI for four pH conditions. Below pH 5, GDBS concentrations are negligible and GMBS formation leads to nearly twice the total S(IV) concentration which would be present in the absence of glyoxal. Above pH 5, GDBS formation leads to even larger S(IV) enrichment factors. In this pH range glyoxal–S(IV) adducts are also a significant reservoir for glyoxal.

Although a rather simplistic set of conditions were chosen, our calculations suggest that glyoxal–S(IV) adduct formation potentially leads to greater scavenging of glyoxal and S(IV) by atmospheric water droplets. Scavenging of SO_2 is particularly enhanced under slightly acidic conditions due to the unique ability of glyoxal to form the dibisulfite adduct.

Acknowledgment. We gratefully acknowledge the Electric Power Research Institute (RP1630-47), the U.S. Public Health Service (ES04635-01), and the Environmental Protection Agency (R811496-01-1) for their financial support.

Registry No. GMBS, 111209-83-7; GDBS, 517-21-5; S(IV), 20681-10-1; glyoxal, 107-22-2.

(32) This Henry's law constant is a minimum value which was experimentally determined by E. Betterton. Details of these experiments will be published elsewhere.

(33) Plum, C. N.; Sanhueza, E.; Atkinson, R.; Carter, W. P. L.; Pitts, J. N. *Environ. Sci. Technol.* **1983**, *17*, 479-84.

A Modeling of the Coesite and Feldspar Framework Structure Types of Silica as a Function of Pressure Using Modified Electron Gas Methods

Mark D. Jackson and G. V. Gibbs*

Department of Geological Sciences, Virginia Tech, Blacksburg, Virginia 24061 *(Received: May 5, 1987; In Final Form: August 5, 1987)*

A theoretical modeling of silica with the coesite and feldspar framework structure types was undertaken as a function of pressure, using the modified electron gas model. As reported for both quartz and cristobalite, an ionic modeling results in more distorted, rigid structures than observed. By use of an ad hoc two-shell bond polarization model to treat covalency, the calculations yield more regular and compliant structures whose bond lengths and angles are in fairly good agreement with experiment. The calculations predict that the feldspar framework of silica is more stable than that of coesite at pressures above 15 GPa.

Introduction

The modified electron gas (MEG) model has been successfully used to generate the structures and stabilities of such monosilicates as the forsterite and spinel polymorphs of Mg_2SiO_4 where the oxide ion is 4-coordinate and the silicate tetrahedron is insular.[1,2] However, this fully ionic model denoted MEG-I, has proven unsuccessful in modeling a monopolysilicate structure like diopside where oxide ions link silicate tetrahedra into a single chain of disiloxy SiOSi groups.[2] It has also proven unsuccessful in modeling the structures and stabilities of the silica polymorphs quartz and cristobalite both of which consist of frameworks of disiloxy groups. As the disiloxy group in these minerals is believed to have appreciable covalent character, Jackson and Gordon[3] modified the MEG model to allow for a polarization of the bridging oxide ion along the SiO bond. This model will be denoted as the MEG-P model. With the development of this model for the oxide ion, they found that the structures and stabilities of quartz and cristobalite can be modeled much better than can be done with the fully ionic MEG-I model. The success of these calculations substantiates the importance of covalency in determining the structures and stabilities of the silica polymorphs. However, a modeling of the forsterite and spinel polymorphs of Mg_2SiO_4 with the MEG-P model yielded structures that are in poorer agreement with the observed ones. Nonetheless, Jackson[1] concluded that a polarization correction is required to generate a satisfactory description of the free energies for the two structures.

In this study, we will use both MEG models to study the structures and stabilities of silica with the coesite and feldspar framework structure types. From a study of the structural relationships for these two, Megaw[4] concluded that the feldspar structure type is unlikely to form because it would require an unusually narrow SiOSi angle of 114.3° which was suggested to destabilize the resulting structure. The present study was undertaken to shed light on the stability of such a framework of silicate tetrahedra as a function of pressure relative to that of coesite. It was also undertaken to learn how well the models generate the zero-pressure structure, the lattice energy, and the bulk modulus of coesite.

A Review of the MEG-P Model

The studies discussed in the Introduction show that the fully ionic MEG-I model provides an inadequate modeling of the structures and energetics of the silica polymorphs quartz and cristobalite whose bonds have appreciable covalent character. To undertake a more reasonable modeling of the feldspar and coesite

(1) Jackson, M. D. PhD. Thesis, Harvard University, 1986.
(2) Post, J. E.; Burnham, C. W. *Am. Mineral.* **1986**, *71*, 142.
(3) Jackson, M. D.; Gordon, R. G. *Phys. Chem. Miner.*, submitted for publication.
(4) Megaw, H. D. *Acta Crystallogr., Sect. B* **1970**, *26*, 261.

0022-3654/88/2092-0540$01.50/0